2022 Basin and Range Earthquake Summit

Utah Geological Survey

Poster Session – Abstracts

GEOLOGY - DAY 1

Poster Session - Abstracts

*Basin and Range Shorelines: Historians of Climate, Geomorphic, and Tectonic Change; *Genevieve Atwood & Natalie A. Hilker, Earth Science Foundation; Tamara Wambeam*

*Are Wasatch Front Earthquakes Preserved in the Great Salt Lake Sedimentary Record?; *Christopher DuRoss, U.S. Geological Survey*

*Rupture in the Mina Deflection: Activation of the Full Range of Transtensional Faults During the 2020 Monte Cristo Range Earthquake Sequence; *Austin Elliott, U.S. Geological Survey*

Preliminary Analysis of Earthquake Geology Input Data for the U.S. National Seismic Hazard Model 2023 Update; *Alex Hatem, U.S. Geological Survey*

Geologic Evidence of Earthquake Behavior on the Eastern Edge of the Basin and Range; *Suzanne Hecker, U.S. Geological Survey*

Detailed Quaternary Fault-Trace Mapping of the Washington, Hurricane, and Sevier Toroweap Fault Zones in Utah and Arizona; *Tyler Knudsen, Utah Geological Survey*

Quaternary Fault Compilation for the INGENIOUS Geothermal Project; *Rich Koehler, University of Nevada, Reno/Nevada Bureau of Mines and Geology*

Insights into Segmentation of the Oquirrh-Great Salt Lake Fault System from Fault Scarp Heights and Lake Bonneville Shoreline Elevations; *Charles Memmott, Utah Valley University*

Paleoseismic History of the Genola North Fault at the West Mountain Site and Connectivity with Utah Lake Faults; *Kristen E. Smith, Utah Valley University*

Lidar Data Reveal Evidence for Late Quaternary Faulting 5km East and Nearly 1000 m Above the Bonneville High Stand, Cutting Glacial Moraines and Talus Cones of the Timpanogos Massif Along the Northern Provo Segment of the Wasatch Fault; *Nathan A. Toké, Utah Valley University*

Preliminary Mapping and Geochronology of the Halfway Gulch Fault, Western Snake River Plain, Idaho; *Brian Gray, Lettis Consultants International, Inc.*

**Digital poster not available. Not all authors provided a digital copy of their poster for inclusion in this meeting proceedings volume.*

BASIN AND RANGE SHORELINES: HISTORIANS OF CLIMATE, GEOMORPHIC, AND TECTONIC CHANGE

Genevieve Atwood, Earth Science Education, genevieveatwood@comcast.net

Natalie A. Hilker, Earth Science Education, nataliehilker@me.com

Tamara Wambeam, wambeam@comcast.net

ABSTRACT

From G.K. Gilbert to the present, Earth scientists have recognized shoreline evidence as storehouses of Earth process information. For open-basin lakes of the Basin and Range, such as paleo-Lake Bonneville or modern Utah Lake, the elevation of the threshold outlet essentially controls the elevation of that lake's shoreline evidence. A lake's threshold is the low place on the basin's rim where a lake crosses into another basin.

Northwestern Utah has many basins, many faults, and ample opportunity to study patterns of shoreline evidence as the interplay of erosion/deposition and tectonics. Interpreting the shoreline evidence of paleolakes may contribute to understanding the tectonics of the Basin and Range.

Patterns of shorelines include series of younger vs. older evidence and progressively higher vs. lower evidence. When threshold elevation lowers, the lake's younger shorelines are lower. When the threshold rises, the younger shorelines are higher. When portions of the floor of the lake drop (basin depresses), the lake level drops and then recovers to its threshold level and leaves a younger shoreline higher than the older. Similar changes in volume will result from lateral spreading of the basin due to Basin and Range extension. The evidence will be younger shorelines higher than older ones. Already-identified series of upward-ramping, upward-younger paleo-shorelines may contribute to an understanding of Basin and Range tectonics as well as lake-level history.

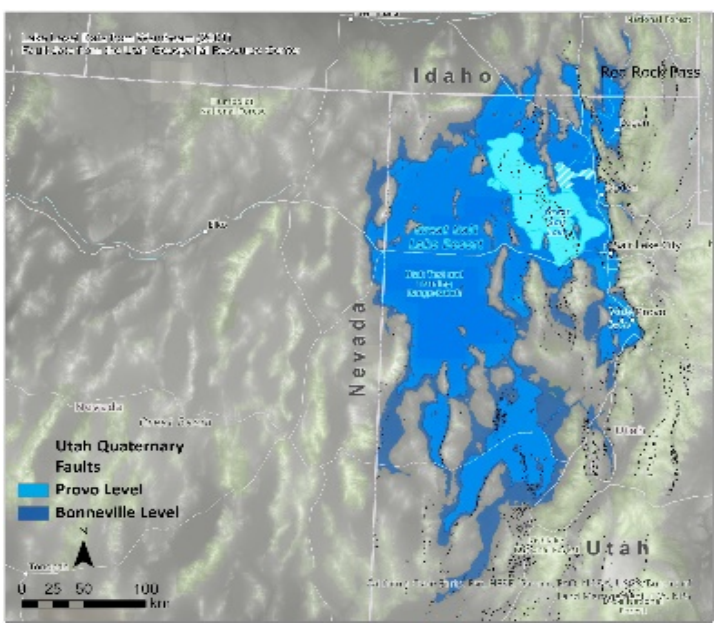

Figure 1. *Location map, Lake Bonneville, Red Rock Pass, Great Salt Lake, and Utah Lake.*

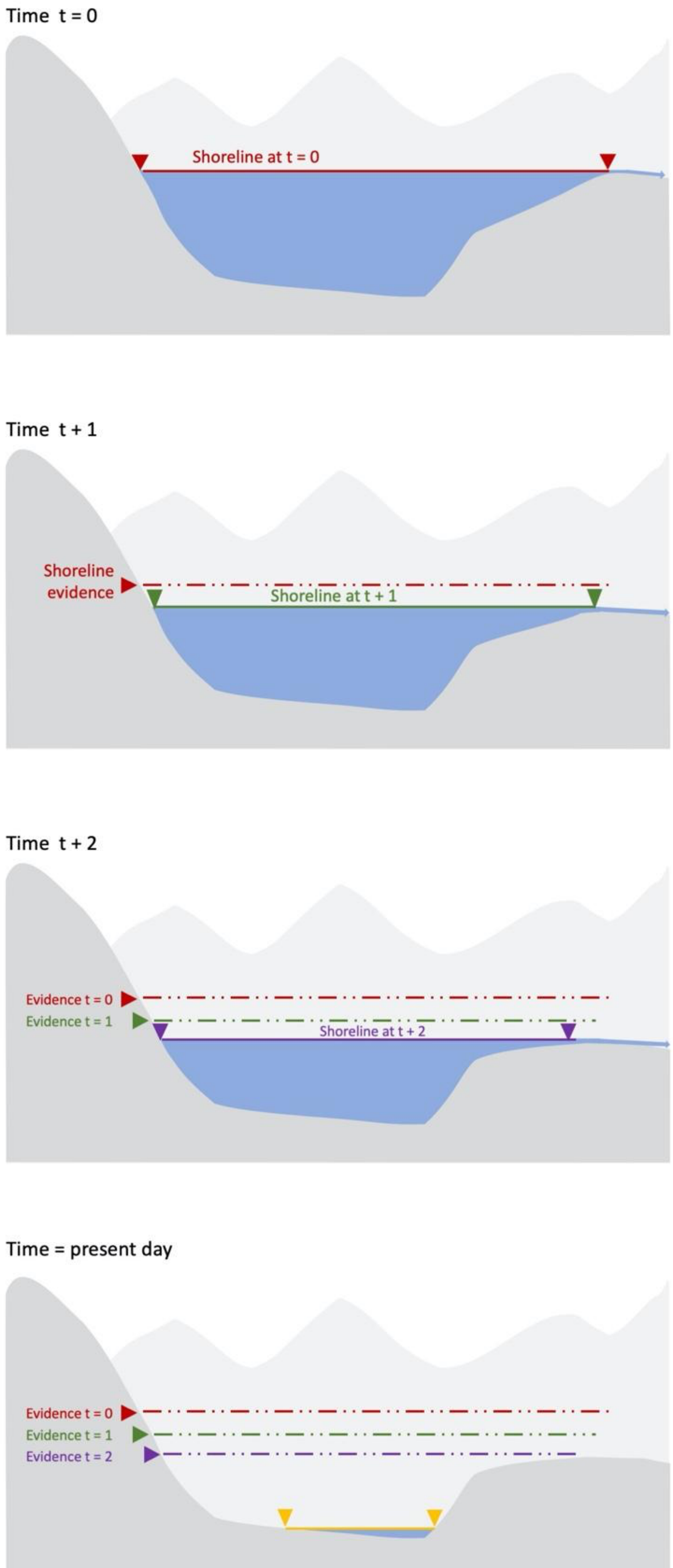

Figure 2. *Scenario 1 - Lower the threshold. In Scenario 1, as a lake's threshold erodes the lake level drops, leaving a pattern of younger, lower shoreline evidence (see figure 2). The erosion could be caused by a catastrophic event such as the Bonneville flood at Red Rock, Idaho or in a slower, steadier, continuous erosional process.*

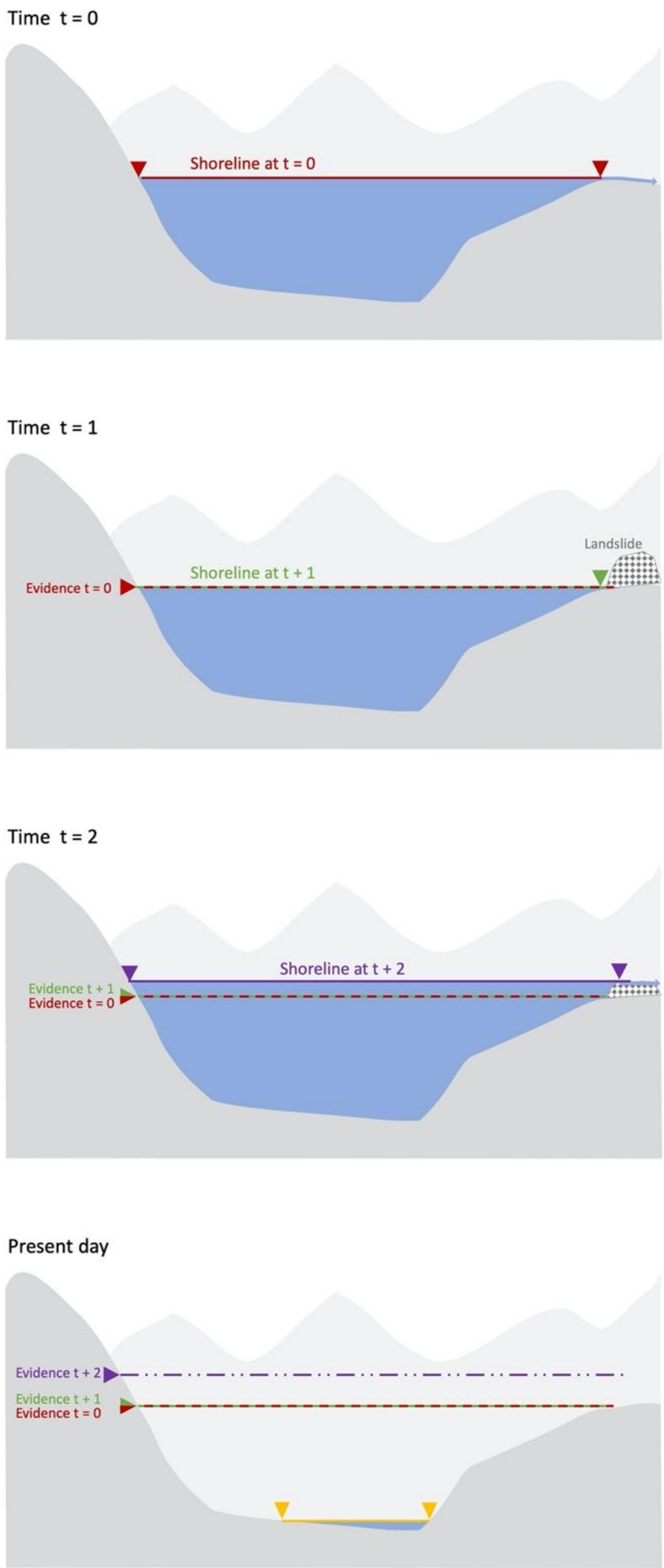

Figure 3. *Scenario 2 - Raise the threshold. In Scenario 2, as a lake's threshold rises, its lake level rises leaving a pattern of younger higher shoreline evidence. The rise of threshold elevation could be caused by a geomorphic process, such as a landslide blocking the outlet, or due to tectonic uplift creating younger, higher shoreline evidence.*

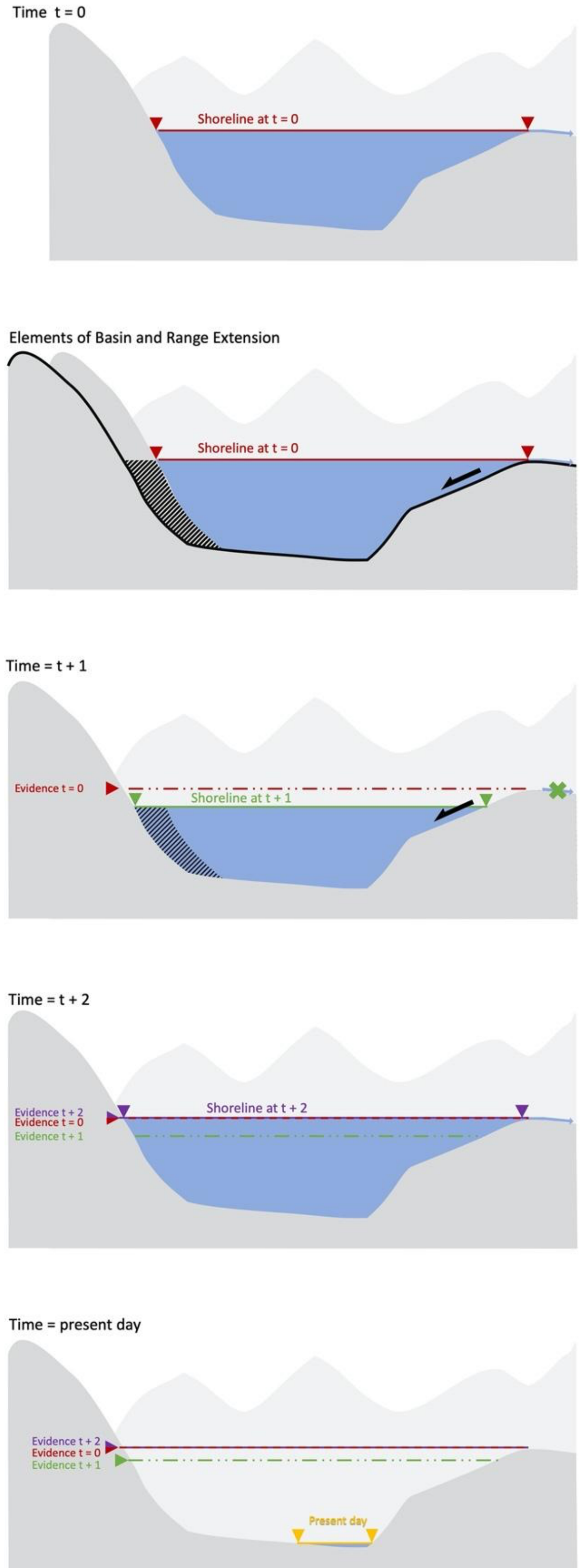

Figure 4. *Scenario 3 - Basin extension. In Scenario 3, the threshold remains steady. Basin and Range extension increases the volume of the lake's basin. Lake level immediately drops below the threshold. The closed-basin lake rises in response to climate until it becomes an open-basin lake overflowing (again) at the threshold. As lake-level rises, it may leave a complex, but generally rising series of younger shorelines between the evidence of t + 1 and t + 2. At t + 2 the lake is a threshold-controlled open basin. Basin extension, creates younger, higher shoreline evidence. This may feel counter intuitive. Patterns of Scenario 3 caused by tectonics resemble those of Scenario 2 caused by geomorphic processes.*

ARE WASATCH FRONT EARTHQUAKES PRESERVED IN THE GREAT SALT LAKE SEDIMENTARY RECORD?

Christopher B. DuRoss, U.S. Geological Survey, cduross@usgs.gov

Daniel S. Brothers, U.S. Geological Survey, dbrothers@usgs.gov

Jessica A. Thompson Jobe, U.S. Geological Survey, jjobe@usgs.gov

Drake M. Singleton, U.S. Geological Survey, dsingleton@usgs.gov

Amanda Rossi, University of Wyoming, arossi2@uwyo.edu

ABSTRACT

Lacustrine paleoseismology, including interpretations from seismic stratigraphy and sediment cores, can yield high-fidelity records of earthquake timing, recurrence, and shaking intensity. Here, we apply these methods to the Great Salt Lake, Utah (GSL; Figure 1) to address questions such as: (1) Are sedimentological records of earthquakes (e.g., mass-transport deposits) present in the GSL record? (2) If so, can on-fault (e.g., Great Salt Lake fault zone) and off-fault (e.g., Wasatch fault zone) earthquake records be differentiated? (3) Did the 2020 M5.7 Magna earthquake (Figure 1) disturb GSL sediments? Our goal is to build on previous work demonstrating as many as six Holocene Great Salt Lake fault earthquakes (Dinter and Pechmann, 2005), compare our results to Wasatch fault zone trench data, and provide an additional, independent record of prehistoric strong shaking along the northern Wasatch Front.

Our study is focused on the south arm of the GSL, along the western shore of Antelope Island (Figure 1). In June–July 2021, we collected 420 line-km of sub-bottom Chirp data, which image the uppermost 20–30 m of unconsolidated lake sediment at 12–15 cm resolution. Guided by interpretations of faulting and related unconformities, we extracted 38 mini hammer cores, which are 6 cm in diameter, 81–189 cm in length, and represent several thousand years of sediment accumulation depending on the site. X-ray computed tomography (CT) density scans and photo logs of the cores reveal finely laminated brine-shrimp fecal pellet silt to fine sand. Along the base of the Great Salt Lake sublacustrine fault scarp near Antelope Island (Figure 1c), the laminated sediments in some cores are truncated by massive, ≤20-cm-thick, normally graded beds. These beds may represent sediment disruption and/or transport during past earthquake shaking. We plan to (1) use the Chirp imagery to examine evidence of Great Salt Lake faulting, stratigraphic growth, and earthquake-related unconformities; (2) document the core sedimentology and relate possible earthquake disturbance horizons to the seismic stratigraphy and historical shaking events such as the Magna earthquake; and (3) evaluate Bayesian models of earthquake timing using charcoal and brine shrimp cysts extracted for radiocarbon dating. These results, when integrated with terrestrial paleoseismic data, will help us resolve the degree to which the GSL acts as a Wasatch Front lacustrine seismograph.

REFERENCES

Baskin, R.L., and Allen, D.V., 2005, Bathymetric map of the south part of Great Salt Lake, Utah, 2005: U.S. Geological Survey Scientific Investigations Map 2894, 1 p.

Dinter, D.A., and Pechmann, J.C., 2005, Segmentation and Holocene displacement history of the Great Salt Lake fault, Utah, *in* Lund, W.R., editor, Basin and Range Province Seismic Hazards Summit II: Basin and Range Province Seismic Hazards Summit II: Utah Geological Survey Miscellaneous Publication 05-2, p. 82–86.

Oviatt, C.G., Madsen, D.B., Miller, D.M., Thompson, R.S., and McGeehin, J.P., 2015, Early Holocene Great Salt Lake, USA: Quaternary Research, v. 84, no. 1, p. 57–68.

Spencer, R.J., Baedecker, M.J., Eugster, H.P., Forester, R.M., Goldhaber, M.B., Jones, B.F., Kelts, K., McKenzie, J., Madsen, D.B., Rettig, S.L., et al., 1984, Great Salt Lake and precursors, Utah: the last 30,000 years: Contributions to Mineralogy and Petrology, v. 86, p. 321–334.

Utah Geological Survey, 2021, Utah Quaternary fault and fold map, https://geology.utah.gov/apps/qfaults, accessed November 2021.

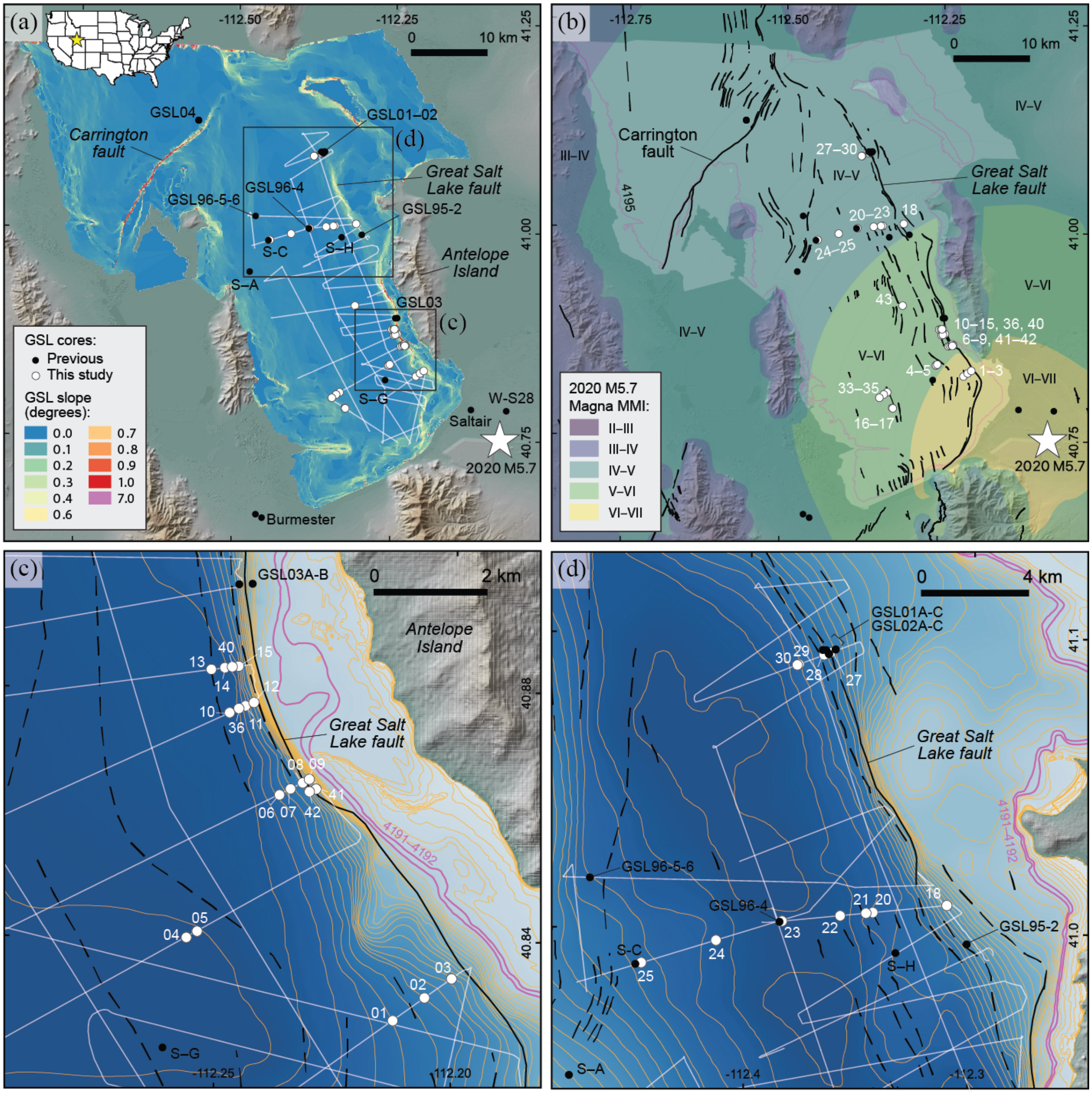

Figure 1. *Seismic-reflection surveys and sediment cores in the south arm of the Great Salt Lake, Utah.* ***(a)*** *Chirp track lines (white lines; this study), previous piston core locations (Spencer and others, 1984; Dinter and Pechmann, 2005; Oviatt and others, 2015), and hammer cores (this study); basemap is slope map derived from 1- foot bathymetric contours (Baskin and Allen, 2005), which highlights the Great Salt Lake and Carrington faults.* ***(b)*** *Hammer core locations compared to ShakeMap-derived shaking intensities for the 2020 M5.7 Magna earthquake; fault traces from the Utah Geological Survey (2021). Pink line shows the 4195 ft shoreline at the time of the earthquake (March 2020).* ***(c)*** *Hammer-core transects across the Great Salt Lake fault scarp near the southern portion of Antelope Island.* ***(d)*** *Piston and hammer cores northwest of Antelope Island. Pink lines show shoreline elevation at the time of this study (June–July 2021).*

RUPTURE IN THE MINA DEFLECTION: ACTIVATION OF THE FULL RANGE OF TRANSTENSIONAL FAULTS DURING THE 2020 MONTE CRISTO RANGE EARTHQUAKE SEQUENCE

Austin Elliott, U.S. Geological Survey, ajelliott@usgs.gov

Seth Dee, Nevada Bureau of Mines and Geology, University of Nevada Reno, sdee@unr.edu

Rich Koehler, Nevada Bureau of Mines and Geology, University of Nevada Reno, rkoehler@unr.edu

Ian Pierce, Department of Earth Sciences, University of Oxford, ian.pierce@earth.ox.ac.uk

Alex Hatem, U.S. Geological Survey, ahatem@usgs.gov

Christine Ruhl, University of Tulsa, cruhl@utulsa.edu

Xiaohua Xu, University of Texas, xiaohua.xu@austin.utexas.edu

ABSTRACT

An array of east-west-striking left-lateral faults transfer transtensional strain from the southern to the central Walker Lane through the Mina Deflection, a ~5,000 km^2 area east of the Mono Basin where active faulting is predominantly conjugate to the main northwest-striking right-lateral shear zone, the Walker Lane. The numerous and relatively short faults within the Mina Deflection suggest smaller maximum magnitudes compared to those possible along the relatively longer adjacent strike-slip faults in the region. However, it has been unclear how individual earthquake ruptures traverse this zone. The May 15, 2020 M_w 6.5 earthquake centered in the Monte Cristo Range (MCR) south of Mina, Nevada, ruptured faults within the Mina Deflection and illuminates how individual earthquake ruptures traverse structurally complex systems such as the Mina Deflection. Integration of observed surface rupture from the field, large-scale deformation from geodesy, and 3D fault geometry from aftershock seismicity reveals that the 2020 MCR earthquake activated left-lateral, right-lateral, normal, and oblique transtensional faults, which represent nearly the full gamut of fault types that comprise the Mina Deflection. The mainshock predominantly ruptured a buried east-west left-lateral fault, apparently the eastward continuation of the mapped Candelaria fault, which experienced only centimeter-scale slip where it was previously recognized at the surface in the west. In the epicentral zone, where left-lateral slip is confined to depths greater than 2 km, north-striking right-normal faults in the overlying alluvial and volcanic deposits show minor slip along reaches above the greatest left-lateral shear below. The largest aftershocks occurred along the conjugate right-lateral Petrified Springs fault located at the eastern end of the rupture. To the west, the mainshock ruptured a pair of oblique left-normal faults that strike more northeasterly, as well as north-south normal faults that connect them. The collection of structures that slipped during this earthquake represent the full range of transtensional fault kinematics present in the Mina Deflection, illuminate subsurface structure, and illustrate how ruptures may navigate among variously oriented smaller faults to produce relatively large-magnitude earthquakes.

PRELIMINARY ANALYSIS OF EARTHQUAKE GEOLOGY INPUT DATA FOR THE U.S. NATIONAL SEISMIC HAZARD MODEL 2023 UPDATE

Alex Hatem, U.S. Geological Survey, ahatem@usgs.gov

Rich Briggs, U.S. Geological Survey, rbriggs@usgs.gov

Ryan Gold, U.S. Geological Survey, rgold@usgs.gov

Camille Collett, ccollett@usgs.gov

ABSTRACT

The U.S. Geological Survey (USGS) plans to release the next update to the U.S. National Seismic Hazard Model (NSHM) in 2023. Here, we describe revisions to the NSHM Fault Sections Database (FSD) and the geologic slip rate database (EQGeoDB) specific to the Intermountain West (IMW). The number of faults included in the FSD across the IMW increased from ~230 fault sections in previous models to ~550 fault sections in 2023 (~140% increase). The increase in the number of faults in the FSD primarily results from relaxing the previous requirement that only faults with direct measurements or estimates of slip rate be included in the NSHM (Figure 1A and B). Where slip rates are not available from the literature, we determined a preferred rate within the Quaternary Fault and Fold Database (QFFD) slip rate bin for a given fault, in conjunction with additional guiding data (e.g., the geodetic strain rate field). These estimated rates, along with field based geologic slip rates, constitute the framework of the geologic deformation model. The EQGeoDB includes over 200 slip rate estimates within the IMW region. Partnerships between USGS and State geological surveys ensured that all available published data were incorporated into the databases.

Preliminary testing of the geologic deformation model shows that, despite adding ~200 fault sections, sub-regions within the IMW exhibit ~ 10%–20% off-fault deformation when comparing geologic and geodetic moment rates within tectonic sub-regions. Fault length across the IMW increased by ~40%, but most of the newly added fault sections have an assigned slip rate of < 0.1 mm/yr. Because the update consisted primarily of short and slow faults compared to previous NSHMs, the total moment summed across the IMW only marginally increased. Rupture rates of earthquakes along individual fault sections show the highest rates of recurrence within the Walker Lane and Wasatch regions, similar to previous NSHMs, with longer rates of recurrence in lower strain regions such as the central Basin and Range Province and the Rio Grande Rift (Figure 1C). This update includes a more complete representation of Quaternary active faults across the IMW; while the aggregate increase in moment rate may be small, site-specific calculations of shaking and hazard curve disaggregations may be influenced by the incorporation of additional fault sources.

A PDF of this poster is available at the following link:

https://ugspub.nr.utah.gov/publications/misc_pubs/mp-177/mp-177-p1.pdf

GEOLOGIC EVIDENCE OF EARTHQUAKE BEHAVIOR ON THE EASTERN EDGE OF THE BASIN AND RANGE

Suzanne Hecker, U.S. Geological Survey, shecker@usgs.gov

David P. Schwartz, U.S. Geological Survey, dschwartz@usgs.gov

Timothy E. Dawson, California Geological Survey, Timothy.Dawson@conservation.ca.gov

ABSTRACT

Paleoseismic and historical observations from the Rocky Mountains provide clues into the source and timing characteristics of large normal-faulting earthquakes along the eastern margin of Basin and Range extension. From a survey of maximum vertical displacements for latest Quaternary and historical surface ruptures, we have found that the ratio of fault slip to fault length, an indicator of static stress drop, is generally largest for structurally immature faults, those with the smallest cumulative displacements (<2 km; Hecker and others, BSSA, 2010). Immature faults are relatively common in the Rocky Mountain region, and their tendency to produce larger-stress-drop earthquakes may reflect greater strength-related roughness and geometric complexity. A recent investigation into the paleoearthquake history of one such fault, the Holocene-activated Bear River fault zone in Wyoming and Utah, yielded age constraints for the initial two events on the fault that fall within a previously recognized mid- to late-Holocene cluster of earthquakes in the southern Middle Rocky Mountains (Hecker and others, Tectonophysics, 2021). This period of elevated strain release on and between widely spaced, low-slip-rate faults, and in particular the apparent close timing of events on the Bear River fault zone and its nearest neighbor, the Rock Creek fault, suggests interrelated fault activity arising from a regionwide redistribution of stress or other perturbation of the stress field. Clustering among networks of similar-slip-rate faults has been interpreted as indicating a strong tendency toward synchronization of seismic cycles and has been recognized elsewhere in intraplate settings, such as for historical and prehistoric earthquake sequences in the central Nevada seismic belt (Scholz, BSSA, 2010). The implications for regional seismic hazard of space-time clustering of high-stress-drop earthquakes are that damaging earthquakes may occur more frequently (or less, depending on where we are situated in the seismic cycle) than indicated by long-term average recurrence estimates and with stronger high-frequency ground motion than may be inferred using general magnitude-fault-length scaling relations. These results point to the need for paleoseismic investigations aimed at characterizing regional fault-group behavior (including possible propensity for high stress-drop earthquakes) and for incorporating the effects of earthquake clustering in time-dependent probabilistic seismic hazard assessments.

A PDF of this poster is available at the following link:

https://ugspub.nr.utah.gov/publications/misc_pubs/mp-177/mp-177-p2.pdf

DETAILED QUATERNARY FAULT-TRACE MAPPING OF THE WASHINGTON, HURRICANE, AND SEVIER/TOROWEAP FAULT ZONES IN UTAH AND ARIZONA

Tyler R. Knudsen, Utah Geological Survey, tylerknudsen@utah.gov

Adam I. Hiscock, Utah Geological Survey, adamhiscock@utah.gov

Jeri Young Ben-Horin, Arizona Geological Survey, jeribenhorin@arizona.edu

Philip A. Pearthree, Arizona Geological Survey, pearthre@arizona.edu

ABSTRACT

The Utah Geological Survey (UGS) and the Arizona Geological Survey (AZGS), with support from the U.S. Geological Survey External Grants Program, completed lidar-based Quaternary fault-trace mapping of the Hurricane, Washington, and Sevier/Toroweap fault zones in southwestern Utah and northeastern Arizona. Where permissible with available lidar coverage, we mapped additional faults adjacent to and possibly structurally related to the Hurricane fault zone, including the Enoch graben, Parowan Valley, and Paragonah faults. These faults pose a significant earthquake hazard to this rapidly urbanizing area of the southwest U.S. In addition to lidar-derived imagery, we used existing geologic mapping, paleoseismic investigations, historical aerial photography, and field investigations to map surface fault traces and to locate scarps amenable to paleoseismic trenching investigations. In Utah, the UGS delineated special-study areas around each fault to encourage recognition, additional investigation, and mitigation of hazardous faults for infrastructure and development. We identified 72 potential trenching sites that may be further evaluated for paleoseismic investigations. Significant discoveries made during our mapping include: (1) some Parowan Valley fault scarps have formed on late Holocene stream alluvium and playa deposits, and likely represent the youngest surface ruptures known in southwest Utah; (2) surface-rupture recency of some Enoch graben faults is obscured where faults exhibit evidence of both seismogenic Holocene surface rupture and aseismic historical creep due to aquifer compaction and ground subsidence related to groundwater mining; (3) the most youthful-appearing scarp (late Pleistocene to Holocene) identified on the main trace of the Sevier/Toroweap fault is superimposed on a significantly older, well-developed obsequent fault scarp, indicating that the average recurrence interval between surface-faulting earthquakes on the Sevier/Toroweap fault in Utah may be relatively long (several tens of thousands of years). Fault-trace geometries and attributes will be published to the UGS *Utah Geologic Hazards Portal*, the AZGS active fault theme on the *Natural Hazards in Arizona Viewer*, and shared with the U.S. Geological Survey for updating the *Quaternary Fault and Fold Database of the United States*.

A PDF of this poster is available at the following link:

https://ugspub.nr.utah.gov/publications/misc_pubs/mp-177/mp-177-p3.pdf

QUATERNARY FAULT COMPILATION FOR THE INGENIOUS GEOTHERMAL PROJECT

Rich Koehler, Nevada Bureau of Mines and Geology, University of Nevada Reno, rkoehler@unr.edu
Zachery M. Lifton, Idaho Geological Survey, zlifton@uidaho.edu
Emily J. Kleber, Utah Geological Survey, ekleber@utah.gov
Tyler Knudsen, Utah Geological Survey, tylerknudsen@utah.gov
Adam Hiscock, Utah Geological Survey, adamhiscock@utah.gov
Stefan Kirby, Utah Geological Survey, stefankirby@utah.gov
Craig dePolo, University of Nevada, Reno, Nevada Bureau of Mines and Geology, cdepolo@unr.edu
James Faulds, Nevada Bureau of Mines and Geology, University of Nevada Reno, jfaulds@unr.edu
Bridget Ayling, Nevada Bureau of Mines and Geology, bayling@unr.edu

ABSTRACT

Thin continental crust, active normal faults, volcanic centers, and permeable rocks make areas of the Great Basin ripe for geothermal potential and production. The U.S. Department of Energy-funded collaborative INnovative Geothermal Exploration through Novel Investigations Of Undiscovered Systems (INGENIOUS) project aims to reduce the exploration risk for hidden geothermal systems in the Basin and Range Province to enhance the understanding of geothermal potential and increase private investment in geothermal energy. As part of the INGENIOUS team, the Nevada Bureau of Mines and Geology, Utah Geological Survey, and Idaho Geological Survey have compiled initial databases for Quaternary faults, seismicity, volcanic deposits, and other relevant information for inclusion in the analysis. Certain structural settings where Quaternary faulting occurs can indicate local permeability and geothermal potential, and therefore fault mapping and rupture parameter data (i.e., slip rates and recency of movement) are important to the project. The INGENIOUS fault database is based on information contained in the *U.S. Quaternary Fault and Fold Database* and individual state fault databases, which contain fault names, mapped scale, slip sense, dip direction, binned categories for slip rate, and age of most recent movement. Starting with these databases, additional data was added, including more discrete ages of the last movement, as well as geologic slip-rate information from published literature. Preferred slip rates developed for the earthquake geology inputs to the 2023 update of the U.S. National Seismic Hazard Model (NSHM) (Hatem and others, 2022) were applied where available. For faults that had no data related to recency of movement and/or slip rate, we used geological observations based on the relative age of geomorphic deposits, fault scarp geomorphology, amount of displacement, and other factors to evaluate these parameters. We will present an updated database of faults, including the recency of faulting and slip rate data, as well as additional fault geometries.

A PDF of this poster is available at the following link:

https://ugspub.nr.utah.gov/publications/misc_pubs/mp-177/mp-177-p4.pdf

INSIGHTS INTO SEGMENTATION OF THE OQUIRRH – GREAT SALT LAKE FAULT SYSTEM FROM FAULT SCARP HEIGHTS AND LAKE BONNEVILLE SHORELINE ELEVATIONS

Charles F. Memmott, Utah Valley University, cfmemmott6@gmail.com

Michael P. Bunds, Utah Valley University, michael.bunds@uvu.edu

ABSTRACT

The Great Salt Lake Fault (GSLF), North Oquirrh Fault (NOF), South Oquirrh Fault (SOF), and Topliff Hills Fault (THF) form a >200-km-long, range-bounding, west-dipping fault system in the eastern Basin and Range near the populous Wasatch Front. The GSLF appears to connect at its south end to NOF, but it is submerged beneath the Great Salt Lake and detail of the structural connection of the two faults is unclear. The NOF and SOF are separated by a structural complexity that obscures their linkage, although tentatively identified fault scarps in the complexity may provide insights. Age constraints for the most recent event (MRE) on each of the four faults are permissive of co-rupture, although age overlap for the NOF and SOF is small and MRE timing on the GSLF and THF are not well known (MRE ages are: GSLF post 10 ka (Dinter and Pechmann, 2014), NOF 4.8–7.9 ka (Olig and others, 1996), SOF 1.3–4.8 ka (Olig and others, 2001), and THF post 12.8 ka (Ward et al., 2019)). We investigate segmentation behavior between the NOF and GSLF, and between the NOF and SOF using the along-strike distribution of surface offset in the MRE and earlier surface-rupturing earthquakes, combined with the elevation of Lake Bonneville shorelines that parallel the NOF and were displaced by surface faulting. 220 measurements of net vertical displacement (offset) were made along the scarps of the NOF and SOF using lidar digital topography. Our preliminary results show that total offset across fault scarps fall into three groups: one-event offsets that range from 2 to 3 m, two-event offsets that range from 5 to 7 m, and three or more event offsets that range from 7 to 10.5 m. One event scarp heights are consistent with trenching results (Olig et al., 1996) and are restricted to sections of fault that displace Bonneville sediments. MRE offset on the NOF increases northward from ~2.4 m in the central portion of the fault to ~3.4 m at its north end near where it connects to the GSLF. A pooled T-test at 95% confidence indicates that this upward trend to the north is statistically significant. This suggests that the MRE on the NOF may have included rupture on at least the southern part of the GSLF, consistent with an estimated >40 km rupture length of the MRE based on offset (Wells and Coppersmith, 1994, Olig et al., 2001) if the rupture terminated to the south at the south end of the NOF (Bunds et al., 2016). Lake Bonneville shorelines in the NOF footwall, which pre-date the MRE and post-date the penultimate event (PE), increase in elevation to the north supporting this hypothesis, although it is difficult to separate isostatic rebound from tectonic effects on shoreline elevation. In contrast, preliminary results indicate that offset in the PE may decrease towards the north end of the NOF, suggestive of a different rupture distribution in that event. Ongoing work includes analysis of offset along the southern NOF and SOF to address segmentation between those faults.

A PDF of this poster is available at the following link:

https://ugspub.nr.utah.gov/publications/misc_pubs/mp-177/mp-177-p5.pdf

PALEOSEISMIC HISTORY OF THE GENOLA NORTH FAULT AT THE WEST MOUNTAIN SITE AND CONNECTIVITY WITH UTAH LAKE FAULTS

Kristen E. Smith, Utah Valley University, krstnwolf92@gmail.com

Nathan A. Toké, Utah Valley University, Nathan.toke@uvu.edu

David R. Johnson, Utah Valley University, David.johnson@uvu.edu

Charles Doug Czajka, Utah Valley University, Doug.Czajka@uvu.edu

Daren T. Nelson, Utah Valley University, nelsonda@uvu.edu

Adam I. Hiscock, Utah Geological Survey, adamhiscock@utah.gov

ABSTRACT

Lidar analysis has led to the discovery of many previously unrecognized active faults, including a 13-km-long discontinuous network of fault scarps running along the west side of West Mountain in Utah County. This westward dipping normal fault, called the Genola North fault, aligns with the Lincoln Point West fault system, within Utah Lake, as well as the Long Ridge fault, located to the south. These faults have been postulated to be coseismic, auxiliary faults to the Provo segment of the Wasatch fault zone. If linked together, these three faults comprise an approximately 40-km-long fault system. Characterizing their seismic hazard is an important consideration for urban development along West Mountain and on Utah Lake. Based upon our lidar interpretation, we selected the West Mountain site (40.1148, -111.8406) due to a ~ 3-m-high fault scarp cutting the Provo shoreline of Lake Bonneville along the northern half of West Mountain. This site is ideal for paleoseismic analysis because of the known geomorphic age for the Provo level shoreline of Lake Bonneville (~ 15 cal ka). A single 30-m-long trench across the fault scarp revealed 20° westward dipping transgressive and regressive lake deposits below a prominent angular unconformity marked by a near horizontal ~ 10-cm-thick carbonate beach deposit. The displacement of the carbonate beach deposit shows a 5 m organic soil-filled fault zone with 3 m of vertical movement. We also observed clear evidence of two ground rupturing earthquakes post Lake Bonneville and at least one rupture close in time to the Bonneville highstand (~18 cal ka). Based on these shoreline ages, we infer an average recurrence rate of 7.5 ka per event and a slip rate of ~0.2 mm/a. Freshwater mollusk shells common to Bonneville basin were sampled for C-14 dating and amino acid racemization to provide age range of the transgressive and regressive lake deposits. Bulk soil samples from fault-derived colluvium should provide additional C-14 dates to help constrain the timing of the penultimate earthquake and the maximum age of the most recent event. Two optically stimulated luminescence (OSL) samples were also collected to help support the radiocarbon dating samples. Other funding is needed to process these OSL samples. This study provides evidence that faults along West Mountain have been active within the Holocene and should be taken into consideration for urban planning in this rapidly growing region.

A PDF of this poster is available at the following link:

https://ugspub.nr.utah.gov/publications/misc_pubs/mp-177/mp-177-p6.pdf

LIDAR DATA REVEAL EVIDENCE FOR LATE QUATERNARY FAULTING 5 KM EAST AND NEARLY 1000 M ABOVE THE BONNEVILLE HIGHSTAND, CUTTING GLACIAL MORAINES AND TALUS CONES OF THE TIMPANOGOS MASSIF ALONG THE NORTHERN PROVO SEGMENT OF THE WASATCH FAULT

Nathan A. Toké, Utah Valley University, nathan.toke@uvu.edu

David R. Johnson, Utah Valley University, 10673213@uvu.edu

Kristen E. Smith, Utah Valley University, krstnwolf92@gmail.com

ABSTRACT

Documenting fault zone width is necessary for characterizing key fault parameters such as slip-rate and earthquake recurrence. The 2014 State of Utah lidar data acquisition provided crucial data for understanding the locations of fault surface rupture hazard along the urban corridor and piedmont of the Wasatch Front; however, the dataset did not span the full width of the Wasatch fault zone. The 2018 Central Utah lidar data demonstrates the importance of collecting wider aperture high resolution topography to fully document fault systems such as the Wasatch. Using lidar derived slopeshade and aspect maps, we identified convincing evidence for fault scarps with multi-meter surface displacements along the high geomorphic features below the west facing cliffs of the Mount Timpanogos massif. Fault surface displacements vary in magnitude with the ages of the geomorphic features that are displaced. Young debris cones are displaced by 2–3 m, recent glacial moraines appear to be displaced by more than 5 m, and older talus cones have displacements ranging from 10 m to more than 20 m. Fault surface breaks extend discontinuously along the massif for at least 10 km and individual fault traces range from ~ 200 m to more than 1500 m in length. The high fault traces are primarily located within the Bridal Veil Limestone member of the Oquirrh Formation and some faults crop out within the Manning Canyon Shale. Our mapping along the northern Provo segment, demonstrates that the surface trace of the Wasatch fault extends across a ~5-km-wide zone extending from near the Bonneville shoreline to the base of the high cliffs of Mount Timpanogos, nearly 1000 meters above the piedmont. The full distribution of fault surface traces between the piedmont and the cliff face is challenging to map due to the presence of numerous landslides within the Manning Canyon Shale and across the fault zone.

A PDF of this poster is available at the following link:

https://ugspub.nr.utah.gov/publications/misc_pubs/mp-177/mp-177-p7.pdf

PRELIMINARY MAPPING AND GEOCHRONOLOGY OF THE HALFWAY GULCH FAULT, WESTERN SNAKE RIVER PLAIN, IDAHO

Brian Gray, Lettis Consultants International, Inc., bgray@lettisci.com

Zachery M. Lifton, Idaho Geological Survey, zlifton@uidaho.edu

ABSTRACT

The Owyhee Mountains fault system (OMFS) is a normal fault system bounding the southwest margin of the western Snake River Plain graben. The Halfway Gulch fault, a section of the OMFS, has a clearly expressed and geomorphically youthful range-front scarp that represents the offset of multiple generations of alluvial-fan and terrace deposits. The Halfway Gulch fault is located less than 100 km south of Boise, Idaho, a metropolitan area with a population of more than 730,000 people. Despite its apparent youthfulness, large uncertainties exist regarding recency of activity, slip rate, geometry, and recurrence interval of the Halfway Gulch fault. Furthermore, this potentially active fault was not included as a seismic source in the 2014 U.S. Geological Survey National Seismic Hazard Model.

We explore the slip history of the Halfway Gulch fault with high-resolution elevation data and satellite imagery, in conjunction with geochronologic dating to bracket the timing of the most recent surface fault rupture and develop constraints on slip rate. Newly collected USGS- and Federal Emergency Management Agency-funded high-resolution lidar data covering the OMFS provide an opportunity to map the Halfway Gulch fault and related Quaternary cover in greater detail than previous mapping efforts completed more than two decades prior. We collected ^{10}Be cosmogenic nuclide depth profile and surface samples, along with optically stimulated luminescence samples to calculate surface exposure ages of faulted and unfaulted deposits that bracket fault activity and provide a basis for slip rate calculations.

Dates for ^{10}Be cosmogenic nuclide and optically stimulated luminescence samples are currently pending for the project. Soil profiles exposed for cosmogenic depth profile pits include well-developed silica-carbonate horizons (Bqm, Bkm duripans) in the youngest faulted alluvial fans. Based on regional soils data, the presence of the silica-carbonate duripan suggests the youngest faulted fans, which are typically displaced 1 to 2 m, are likely several hundred thousand years old or older. An exposure pit excavated into the oldest unfaulted fan exposed soils that lack the well-developed duripan of the older faulted surface. Stage I to Stage II carbonate development in this younger fan indicates this oldest unfaulted surface is significantly younger than the faulted surface. Following delivery of cosmogenic sample dates for this younger surface, we intend to explore the structural and temporal relations of the Halfway Gulch and adjacent Water Tank faults that collectively define a geomorphically youthful section of the OMFS.

A PDF of this poster is available at the following link:

https://ugspub.nr.utah.gov/publications/misc_pubs/mp-177/mp-177-p8.pdf

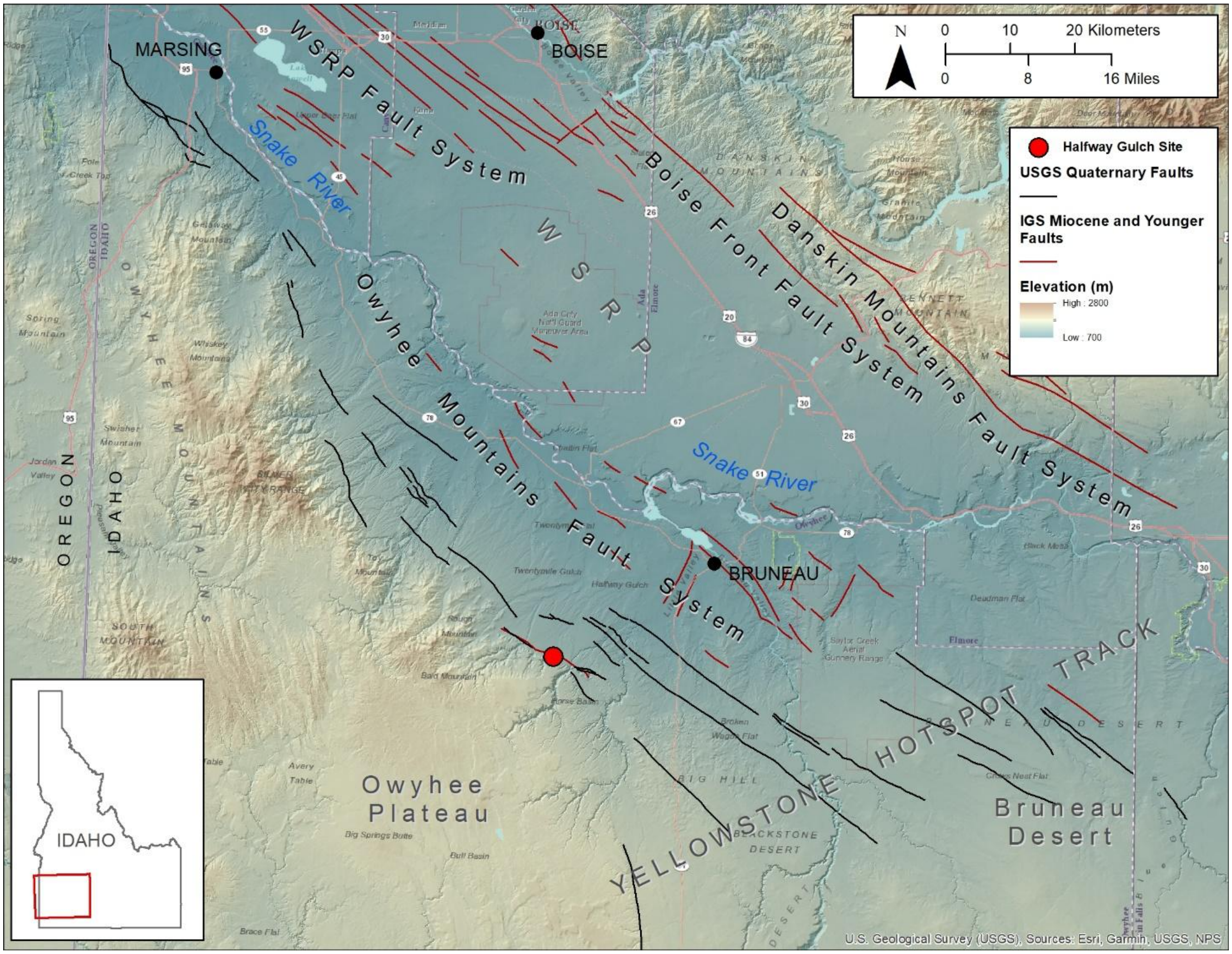

Figure 1. *Neotectonic map of southwestern Idaho showing faults of the Western Snake River Plain.*

SEISMOLOGY - DAY 2

Poster Session - Abstracts

The Colorado Geological Survey Seismic Network and Colorado's Seismically Active Regions; *Kyren Bogolub, Colorado Geological Survey*

Coulomb Stress Change from the March 18, 2020, Magna M_w 5.7 Earthquake and Implications for the Wasatch Fault Seismic Hazard; *Michael Bunds, Utah Valley University*

Double Beamforming Ambient Noise Tomography of the East Bench Fault Using a Temporary Linear Array; *Konstantinos Gkogkas, University of Utah*

*Seismic Profiling Across the Eglington and Frenchman Mountain Faults, Las Vegas, Nevada; *Lee Liberty, Boise State University*

Recent Developments in Seismic Monitoring in New Mexico; *Mairi Litherland, New Mexico Bureau of Geology*

*Modeling Aftershock Sequences in the Eastern Intermountain West; *Kristine Pankow, University of Utah Seismograph Stations*

A Logic Tree for the Subsurface Geometry of the Salt Lake City Segment of the Wasatch Fault in Light of the 2020 Magna, Utah Earthquake; *Jim Pechmann, University of Utah*

*Four decades of Seismic Swarm Activity in the Transition Zone between Basin-and-Range and Colorado Plateau, Central Utah; *Gesa M. Petersen, University of Utah Seismograph Stations*

*Structural Immaturity and Tectonic Implications of the 2020 M_w 6.5 Monte Cristo Range Earthquake, Nevada: Evidence from Near-Field and Far-Field Observations; *Israporn Sethanant, University of Victoria*

*Relocating the Utah Magna Aftershock Sequence Using NonLinLoc Source-Specific Station Terms, and Waveform Similarity; *Daniel Wells, University of Utah*

The Implications of a Listric Wasatch Fault for Seismic Hazard Along Utah's Wasatch Front; *Ivan Wong, Lettis Consultants International, Inc.*

Interseismic Strain Accumulation Across the Central Basin and Range: Implications for Southern Nevada Seismic Hazard; *Zachary M. Young, Nevada Geodetic Laboratory*

Investigating the 3D Basin Structure of Salt Lake Valley Using Surface Waves Recorded by the Magna Aftershock Nodal Array; *Qicheng Zeng, University of Utah*

**Digital poster not available. Not all authors provided a digital copy of their poster for inclusion in this meeting proceedings volume.*

THE COLORADO GEOLOGICAL SURVEY SEISMIC NETWORK AND COLORADO'S SEISMICALLY ACTIVE REGIONS

Kyren Bogolub, Colorado Geological Survey, kbogolub@mines.edu

Matt Morgan, Colorado Geological Survey, mmorgan@mines.edu

ABSTRACT

The Colorado Geological Survey Seismic Network (CGSSN) consists of eight permanent seismic stations. The network is primarily used to locate small magnitude and induced earthquakes throughout the state. We will be presenting on the status of the current network and our goals for the future of the CGSSN in the context of the seismically active regions of the state. This will include a focus on historical earthquakes of Colorado as well as modern earthquake catalogs. We will also highlight some of the lessons we have learned in developing the network and the collaborations that have made the network possible.

A PDF of this poster is available at the following link:

https://ugspub.nr.utah.gov/publications/misc_pubs/mp-177/mp-177-p9.pdf

COULOMB STRESS CHANGE FROM THE MARCH 18, 2020, MAGNA M_W 5.7 EARTHQUAKE AND IMPLICATIONS FOR WASATCH FAULT SEISMIC HAZARD

Michael P. Bunds, Utah Valley University, Michael.Bunds@uvu.edu

Michael A. Stearns, Utah Valley University, MStearns@uvu.edu

ABSTRACT

The March 18, 2020, M_w 5.7 Magna earthquake occurred 18 km west of the surface trace of the Salt Lake City (SLC) segment of the west-dipping Wasatch fault (WF) in the populous Salt Lake Valley on the eastern edge of the Basin and Range. The SLC segment is capable of producing a > M7 earthquake and it is late in its seismic cycle (Working Group on Utah Earthquake Probabilities, 2016). Published source mechanics and analysis of the distribution of aftershocks show the Magna earthquake was caused by normal-oblique slip on a fault that dips 30° ± 10° west (University of Utah Seismograph Stations, 2020; Pang and others, 2020). To our knowledge, this is the first recorded moderate to large earthquake on a normal fault that dips ~30° or less in the Basin and Range. Furthermore, if the WF is listric and dips ~30° W in the subsurface, then the earthquake likely occurred on the down-dip extension of it (such as, Pang and others, 2020). To address possible impacts of the Magna earthquake on WF seismic hazard, we calculate Coulomb stress change imparted by slip in the earthquake on receiver faults that model the SLC segment of the WF and estimate changes in future earthquake probability from the stress changes. Our results indicate that if the WF is listric, then Coulomb stress on it has increased significantly no matter if the Magna earthquake occurred on it. In contrast, if the WF dips more than about 45° in the subsurface and lies to the east of the Magna earthquake source at depth then Coulomb stress and seismic hazard on it probably was reduced. For the scenario that the Magna earthquake occurred on the down-dip extension of the WF, we estimate Coulomb stress increased ~1 b average over ~290 km^2 of area on the SLC segment of the WF. These results are similar to estimated increases prior to large earthquakes apparently triggered by slip on nearby faults (e.g., Hodgkinson et al., 1996; Nalbant et al., 2005; Toda and Stein, 2020). We apply the method of Stein and others (1997) to estimate the change in future earthquake probability on the WF that could be expected from the Coulomb stress changes. In this method, both transient and long-term effects of Coulomb stress change are incorporated into standard, existing estimates of conditional probability. The transient effect uses rate-and-state friction theory (Dieterich, 1994) to estimate a transient increase in earthquake frequency based on the Coulomb stress change and observed activity increases following other earthquakes. To include the long-term effect, the Coulomb stress change is equated to a length of time to accumulate the same stress change by tectonic loading and then shortening the mean recurrence time accordingly. Our results suggest the Magna earthquake may have increased the 10-year conditional probability of a surface-rupturing earthquake on the WF by a factor of 1.5 to 3.3 (i.e., from ~1.5% to ~2.1%–5%), and the 50-year conditional probability by factor of 1.1 to 1.5 (i.e., from ~7.5% to ~8.5%–12%) relative to existing conditional probability estimates (WGUEP, 2016).

A PDF of this poster is available at the following link:

https://ugspub.nr.utah.gov/publications/misc_pubs/mp-177/mp-177-p10.pdf

DOUBLE BEAMFORMING AMBIENT NOISE TOMOGRAPHY OF THE EAST BENCH FAULT USING A TEMPORARY LINEAR ARRAY

K.Gkogkas, University of Utah, kos.gkogkas@utah.edu

F.-C. Lin, University of Utah, FanChi.Lin@utah.edu

A.A. Allam, University of Utah, amir.allam@utah.edu

ABSTRACT

We provide new constraints on the shallow structure of the East Bench segment of the Wasatch Fault System by exploiting continuous data recorded from a month-long temporary linear array of 32 nodal stations deployed along 1700 South in Salt Lake City. We cross-correlate the ambient noise records and extract Rayleigh wave signals in the period range 0.4 s to 1.1 s. We apply double beamforming, enhance the signal, measure period-dependent Rayleigh wave phase velocities and construct a 2-D profile. We invert the 1-D phase velocity dispersion curve at each beam center by adapting an uncertainty-weighted least-squares inversion scheme and combine all inverted 1-D Vs models to obtain a pseudo-2D Vs model for the area, mostly sensitive at the upper 400 m beneath the array. The resulting Vs model exhibits faster velocities to the east and slower velocities to the west, in good agreement with the expected thickening of sedimentary deposits towards the center of the basin. Moreover, a 400 m-wide low-velocity zone narrowing with depth is observed proximate to the surface trace of the East Bench fault, suggesting the presence of a fault damage zone. The proposed geometry of the damage zone is asymmetric, being wider on the hanging wall and with greater velocity reduction. Our results provide important information regarding the shallow structure and mechanics of the Wasatch Fault System and for the seismic hazard assessment in Salt Lake City. Furthermore, the good correlation between our model features and the local geologic and tectonic structures encourages more extensive future applications of ambient noise imaging in Salt Lake City.

A PDF of this poster is available at the following link:

https://ugspub.nr.utah.gov/publications/misc_pubs/mp-177/mp-177-p11.pdf

SEISMIC PROFILING ACROSS THE EGLINGTON AND FRENCHMAN MOUNTAIN FAULTS, LAS VEGAS, NEVADA

Lee M. Liberty, Boise State University, lliberty@boisestate.edu

Seth M. Dee, Nevada Bureau of Mines and Geology, University of Nevada Reno, sdee@unr.edu

ABSTRACT

We explore the geometry and history of motion of two fault systems that extend through the Las Vegas metropolitan area. The 11-km-long intrabasin Eglington fault, part of the Las Vegas Valley fault system, is expressed as a surface warp in Quaternary sediments. Hypotheses regarding the mechanisms responsible for Eglington warp formation include: coseismic warping, climatically modulated tectonic displacement, and differential sediment compaction. Results from a new 1.5-km-long seismic profile reveal that the warp and associated scarps are underlain by a broad deformation zone. From 200 to 1000 m depth, reflectors are truncated, tilted, and offset, interpreted as a high-angle fault zone. The association of the surficial warp with a subsurface fault zone extending to such depths is consistent with a tectonic origin. The upper 200 m of the profile images tilted and offset reflectors with dips and displacements that are discordant from the underlying reflections. A reflection image with a hand-pulled seismic streamer, with a focus on the upper 10s of meters, is consistent with deformation extending into the shallowest sediments. The discordant, near-surface deformation is at the stratigraphic levels most influenced by late Pleistocene climatically driven ground-water level changes. These results suggest that both tectonic and non-tectonic processes may contribute to deformation along the Eglington fault.

The Frenchman Mountain fault system is a 33-km-long, arcuate (convex-west), west-dipping, range-bounding normal and dextral-oblique fault on the eastern side of the Las Vegas metropolitan area. The main Quaternary trace of the northern section of the fault system is expressed as a zone of scarps in alluvial-fan surfaces. Two new seismic profiles across this fault section illustrate its subsurface geometry. The main Quaternary scarp, previously identified as a ~60° - 70° west-dipping fault, intersects a prominent ~30° west-dipping reflector on both profiles that we interpret as a low-angle normal fault that separates late-Cenozoic sediments from older bedrock. The high-angle fault does not measurably offset the low-angle fault at the resolution of the profiles, thus constraining total vertical displacement to less than 10s of meters. Exposed on the footwall side of the Quaternary fault scarp, is a 35° west-dipping fault that may correlate with the low-angle fault imaged in the profile, further constraining total vertical displacement across the steeply dipping fault to < 10s of meters. Imaged on the Owens Avenue profile are strata of probable Miocene age in the low-angle fault's hanging wall that are warped into a rollover anticline geometry and faulted against Precambrian basement. A prominent gravity gradient immediately west of our profiles suggests an additional high-angle fault bounds the deepest part of the Las Vegas basin and accommodated the bulk of late-Cenozoic basin formation.

RECENT DEVELOPMENTS IN SEISMIC MONITORING IN NEW MEXICO

Mairi Litherland, New Mexico Bureau of Geology and Mineral Resources, mairi.litherland@nmt.edu

Amy Record, New Mexico Bureau of Geology and Mineral Resources, amy.record@nmt.edu

ABSTRACT

New Mexico experiences a moderate level of naturally occurring seismicity, primarily along the Rio Grande Rift that runs N-S along the center of the state, along with induced seismicity in oil and gas producing basins. The New Mexico Tech Seismological Observatory (NMTSO) began recording earthquakes in New Mexico in 1960 at station SNM, 5 km west of Socorro, New Mexico. Since then, the network has expanded over time, and at present the NMTSO operates a total of 23 stations to monitor seismic activity throughout the state, with a mix of single-component short-period and three-component broadband stations. The University of New Mexico, Los Alamos National Laboratory, the U.S. Geological Survey, and the State of Texas maintain additional stations in and around New Mexico. A number of additional seismic stations have been installed in just the past several years as a response to the rapid increase in induced seismicity in New Mexico, particularly in the Permian Basin in southeastern New Mexico. The NMTSO has also begun using Seiscomp for routine earthquake processing as well as incorporating machine learning methods for earthquake detection. These increased capabilities have been essential to assisting regulatory agencies with strategies to manage induced seismicity and informing the public about seismic hazard in the state. Ongoing projects are using template matching and machine learning to improve catalog completeness, and earthquake relocation methods to improve location accuracy. Future projects will examine the association between fluid injection/fracking and seismicity and expand network capabilities in parts of the state that currently lack monitoring coverage.

A PDF of this poster is available at the following link:

https://ugspub.nr.utah.gov/publications/misc_pubs/mp-177/mp-177-p12.pdf

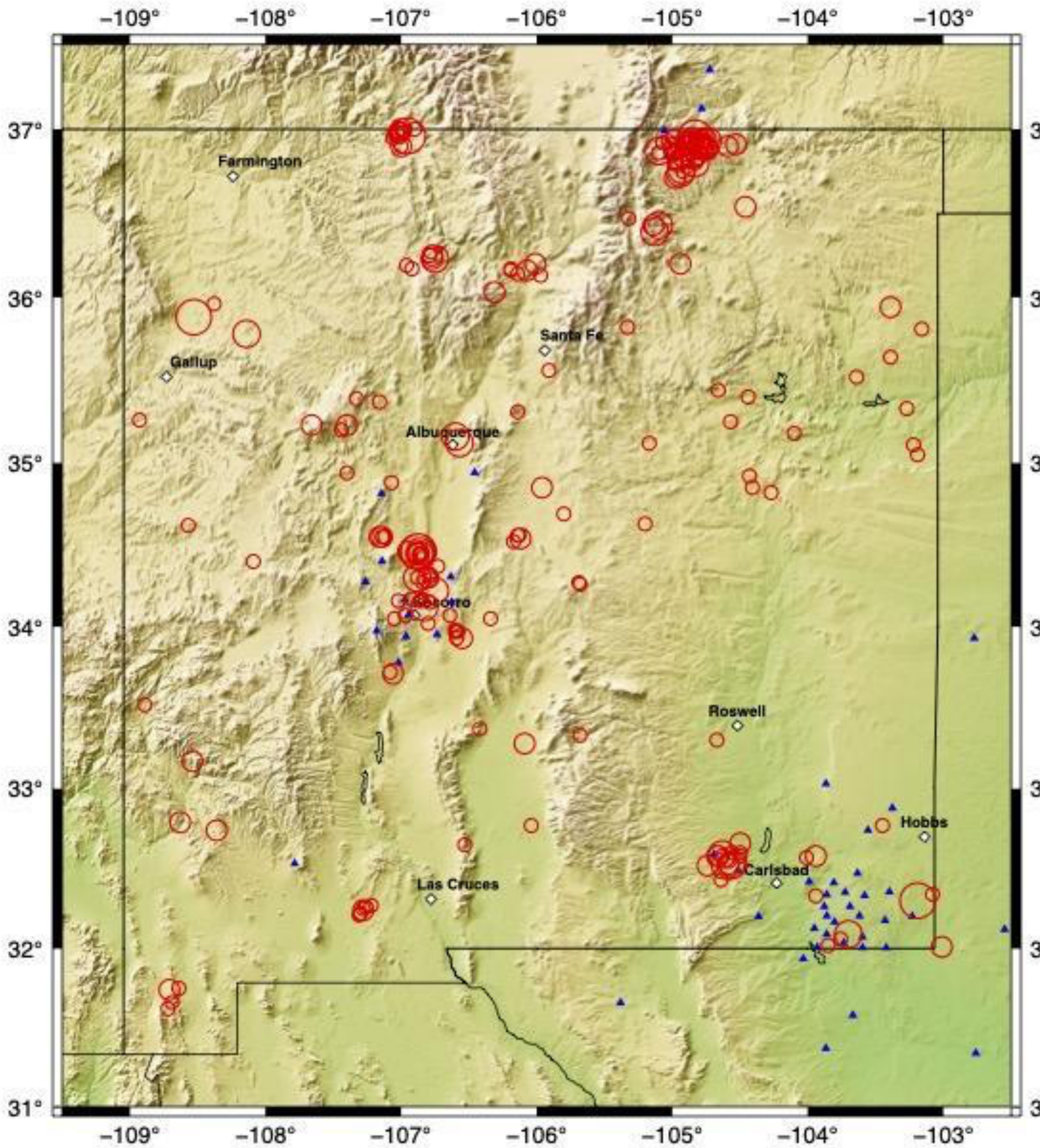

Figure 1. *Earthquakes >M3.0 from the NMTSO and USGS catalogs from 1962–2021; the magnitude of the event is represented by the size of the circle (ranging from M3 to M5). Publicly available seismic monitoring stations in New Mexico and selected stations from neighboring states are represented by blue triangles.*

MODELING AFTERSHOCK SEQUENCES IN THE EASTERN INTERMOUNTAIN WEST

Maria Mesimeri, Swiss Seismological Service, ETH, maria.mesimeri@sed.ethz.ch

Kristine L. Pankow, University of Utah Seismograph Stations, kris.pankow@utah.edu

ABSTRACT

Operational aftershock forecasting (OAF) is a relatively new product provided by the U.S. Geological Survey (USGS). It has been shown that aftershock model parameters, such as productivity and decay vary regionally. In the USGS models, the Intermountain West (IMW) is grouped into a larger area that includes much of the western U.S. In this study, we acquire earthquake catalogs from the University of Utah Seismograph Stations and the Montana Bureau of Mines and Geology (MBMG), combined with sequence specific catalogs for M ≥ 5.0 mainshocks. Using the UUSS and MBMG catalogs, we first identify earthquake sequences (Mmax ≤ 5.0) that are clustered in space and time, and then sort the sequences into mainshock-aftershock sequences and earthquake swarms based on high order statistics of the moment release history (i.e., skewness and kurtosis). For each mainshock-aftershock sequence, both from the clustering analysis and the sequence specific catalogs, we model the productivity and decay properties. We find that the aftershock sequences differ from the model currently used in USGS OAF. Additionally, we report that there are differences in model parameters for different magnitude ranges, and therefore we propose three magnitude-dependent models. Interestingly, for the largest magnitude range, M > 6, the productivity is much less than what is found for the smaller magnitude events. Furthermore, we find that many of the earthquake sequences identified in the UUSS and MBMG catalogs are earthquake swarms. In Utah, the swarms are more geographically isolated, but in Montana occur more regionally. This result underscores the necessity of OAF for earthquake swarms, especially for regions where earthquake swarms are frequent, like the eastern IMW.

A LOGIC TREE FOR THE SUBSURFACE GEOMETRY OF THE SALT LAKE CITY SEGMENT OF THE WASATCH FAULT IN LIGHT OF THE 2020 MAGNA, UTAH EARTHQUAKE

James C. Pechmann, University of Utah, james.pechmann@utah.edu

Ivan G. Wong, Lettis Consultants International, wong@lettisci.com

Christopher B. DuRoss, U.S. Geological Survey, cduross@usgs.gov

Michael D. Hylland, Utah Geological Survey, mikehylland@utah.gov

Anthony J. Crone, U.S. Geological Survey (retired), ajcrone65@gmail.com

Stephen F. Personius, U.S. Geological Survey (retired), greenmtn1@yahoo.com

Adam P. McKean, Utah Geological Survey, adammckean@utah.gov

Walter J. Arabasz, University of Utah, wjax99@gmail.com

David P. Schwartz, U.S. Geological Survey, dschwartz@usgs.gov

Susan S. Olig, Olig Seismic Geology, oligseismicgeo@gmail.com

William R. Lund, Utah Geological Survey (retired), williamlundugs@gmail.com

David A. Dinter, University of Utah, david.dinter@utah.edu

ABSTRACT

The 2020 M_w 5.7 Magna earthquake was the largest, and most damaging, earthquake to occur in Utah since the 1992 M_w 5.5 St. George earthquake. Long-period regional waveform modeling, in combination with the aftershock distribution, indicates that the Magna mainshock occurred 10.5 ± 2 km below the northwestern Salt Lake Valley on an oblique-normal fault dipping 34°–39° W (Figure 1a). Published studies have interpreted the mainshock rupture to be on the Salt Lake City segment of the Wasatch fault (SLCS), which dips 70° WSW along the nearest surface trace 15 km ENE of the epicenter. This interpretation implies a listric geometry for the fault, i.e., a dip that decreases downward. The existence of the east-dipping West Valley fault zone (WVFZ), located 3–10 km W of the northern half of the SLCS, provides independent evidence of a listric geometry for this part of the SLCS. A decrease in dip on the SLCS below where it intersects the WVFZ would permit both of these faults to slip without offsetting each other, forming a large-scale backtilt graben system. The estimated ratio between the vertical slip rates on the WVFZ and the SLCS is 0.09–0.42, which provides a weak model-dependent constraint on the dip change of the SLCS. Nevertheless, even if a listric model for the northern SLCS is assumed, the precise subsurface fault geometry remains uncertain. We also cannot rule out the possibility that the Magna earthquake occurred on a west-dipping subsidiary fault in the hanging wall of the SLCS.

Here, we present a logic tree of four possible models for the subsurface geometry of the SLCS that are consistent with data from the Magna earthquake and the WVFZ. In all four models the southern half of the SLCS (the Cottonwood section) has a planar geometry with an asymmetric weighted west dip distribution of 35°(0.3)–50°(0.5)– 65°(0.2). This planar model is like models formerly used for the entire Wasatch fault, but with slightly more weight on the lower-angle dips. For the northern half of the SLCS (the Warm Springs and East Bench sections) the four models (with weights) are: (1) Planar, with the same dip distribution as the Cottonwood section (0.2); (2) Listric, with the possible added complication of a "ramp-flat" geometry around the mainshock rupture (0.4, Figure 1b); (3) Minimally listric (0.2, Figure 1c); and (4) Deep listric (0.2, Figure 1d). The Magna earthquake is on or near the SLCS in the 35°-dipping branch of Model 1 and in Models 2 and 3, which have a combined weight of 0.66; in Model 4 and in the other branches of Model 1, this earthquake is on a subsidiary fault in the SLCS hanging wall. The new logic tree incorporates a plausible range of uncertainties in the subsurface geometry of the SLCS. Using this logic tree for probabilistic seismic hazard analyses, instead of the previously favored planar models with dips of 50° ± 15°, will increase the predicted ground shaking hazard in the northwest Salt Lake Valley because of the shorter average distances to the SLCS.

A PDF of this poster is available at the following link:

https://ugspub.nr.utah.gov/publications/misc_pubs/mp-177/mp-177-p13.pdf

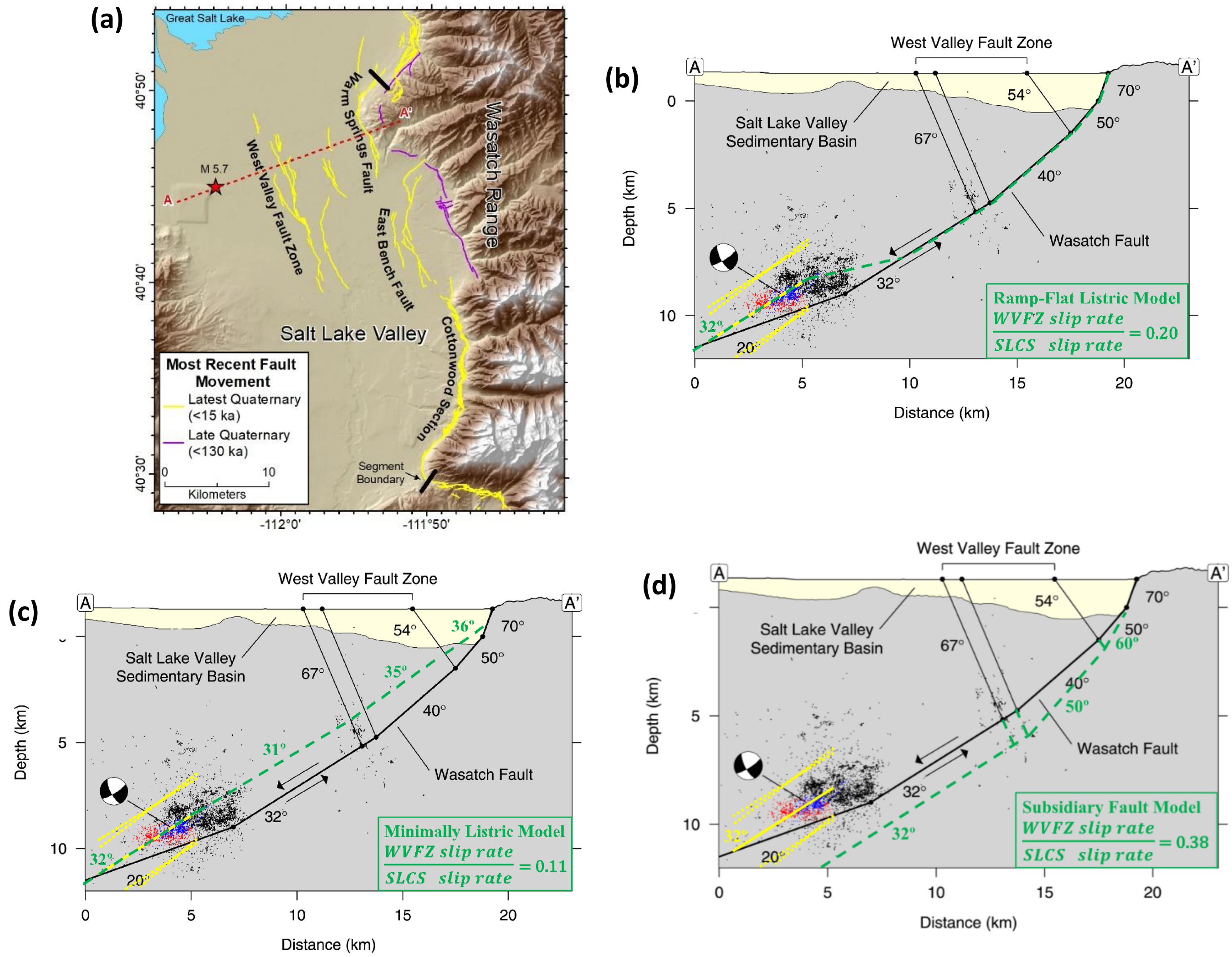

Figure 1. (a) *Map showing late Quaternary fault traces from the Utah Geological Survey, the epicenter of the M_w 5.7 Magna earthquake (red star), and the line of the cross sections in the other panels.* ***(b)–(d)*** *Hypocentral cross sections of the Magna sequence from March 18 through April 30, 2020, modified from Figure 3 of Pang and others (2020, GRL, e2020GL089798). The solid black lines show Pang et al.'s interpretation of the subsurface fault geometry. The dashed green lines show alternative subsurface geometries for the Wasatch fault (Models 2–4). The green box in each panel shows the predicted slip rate ratio between the West Valley fault zone and the Salt Lake City segment for the dashed green fault model. The dotted yellow lines are projections of the W-dipping nodal planes from four mainshock moment tensor solutions. Each projection passes through the centroid depth at the mainshock epicenter and extends ~1.5 km updip and ~4 km downdip from there, consistent with source studies. The solid yellow line is the projection of the W-dipping nodal plane of the University of Utah solution, shifted to 9 km depth at the epicenter.*

FOUR DECADES OF SEISMIC SWARM ACTIVITY IN THE TRANSITION ZONE BETWEEN BASIN AND RANGE AND COLORADO PLATEAU, CENTRAL UTAH

Gesa M. Petersen, University of Utah Seismograph Stations, gpetersen@seis.utah.edu

Katherine Whidden, University of Utah Seismograph Stations, katherine.whidden@utah.edu

Kristine L. Pankow, University of Utah Seismograph Stations, Kris.Pankow@utah.edu

ABSTRACT

Central Utah is situated in the transition zone between the Basin and Range province and the Colorado Plateau. The complex geotectonic setting is not only shaped by horst and graben structures related to the east-west extension, but also by transecting east-west-striking transverse structures, Mesozoic thrust fault systems, Cenozoic to Quaternary volcanism, hot springs, and increased heat flow. Seismic activity is mostly of low to moderate magnitudes, but includes a number of historical large and destructive events.

Seismically, central Utah is considered part of the Intermountain Seismic Belt, spanning from southern Nevada and northern Arizona to northwestern Montana with dominant normal faulting and additional strike-slip faulting mechanisms. Seismic swarms in central Utah have been observed by different authors in the past and attributed to either normal faults that are associated with the divides between basin and ranges and/or to fluid migration. Over the last four decades, the seismic station coverage in the area increased significantly, resulting in decreased detection thresholds and increased location accuracy. Here, we revisit the entire digital seismic catalog of the University of Utah Seismograph Stations (1981–2022) and perform a statistical analysis of seismic sequences within the catalog. We evaluate typical features of swarms in the area and interpret them in relation to newly derived focal mechanisms and geotectonic background information.

Furthermore, we perform in-depth analyses of four interesting seismic sequences, namely the 2011 Circleville seismic sequence, a seismic swarm in the Mineral Mountains in 2020, a massive seismic swarm close to Milford in 2021, and a small seismic swarm in the Sevier Valley in February 2022. By using advanced techniques for event detections, relocations, full waveform-based moment tensor inversions, and waveform similarity-based clustering, we obtain new insights into the process of the swarms and the geometry of activated faults. We infer and discuss possible triggering mechanisms and attempt to integrate our findings into the larger seismo-geo-tectonic context of the transition zone.

STRUCTURAL IMMATURITY AND TECTONIC IMPLICATIONS OF THE 2020 M_W 6.5 MONTE CRISTO RANGE EARTHQUAKE, NEVADA: EVIDENCE FROM NEAR-FIELD AND FAR-FIELD OBSERVATIONS

Israporn Sethanant, University of Victoria, isethanant@uvic.ca

Edwin Nissen, University of Victoria, enissen@uvic.ca

Léa Pousse-Beltran, Université Grenoble Alpes, Université Savoie Mont Blanc, CNRS, IRD, Université Gustave Eiffel, ISTerre, lea.pousse@univ-grenoble-alpes.fr

Eric Bergman, Global Seismological Services, bergman@seismo.com

Harley M. Benz, United States Geological Survey, benz@usgs.gov

Ian Pierce, Department of Earth Sciences, University of Oxford, ian.pierce@earth.ox.ac.uk

ABSTRACT

The 2020 M_w 6.5 Monte Cristo Range earthquake (MCRE) is the largest instrumental event in the Mina deflection, a pronounced east-trending stepover zone linking northwest-striking faults within the Walker Lane. The MCRE mostly ruptured previously unmapped faults, motivating us to characterize the earthquake behavior along poorly expressed, likely structurally-immature faults within a region of highly distributed deformation. We use Sentinel-1B Interferometric Synthetic Aperture Radar (InSAR) data and regional Global Navigation Satellite System (GNSS) coseismic offsets to model the causative faults and coseismic slip distribution of the MCRE. Modeling results show that two faults yield the lowest misfit between data and model. The eastern fault strikes east-northeast, has dominant left-lateral motion, and obliquely crosses the northeast-striking western fault that exhibits a large extensional component. Maximum slip of 1 m occurs on the eastern fault plane at 8–10 km depth, but less than 0.1 m of slip reaches the surface, indicating a pronounced shallow slip deficit of 91%. We also relocate 197 hypocenters of the MCRE sequence using *mloc* software. The calibrated relocation indicates that the mainshock initiated at 9 km depth and aftershock focal depths range from 1 to 11 km, helping constrain the local seismogenic thickness and the bottom depth of our geodetic slip model. Most aftershocks are located south of the surface projection of the model faults, supporting the southward dip inferred from InSAR and GNSS modeling, though many likely lie off the mainshock fault plane within the surrounding volume. In addition, we calculate regional moment tensor solutions for the 90 best-recorded events. The aftershocks exhibit a wide variety of normal and strike-slip mechanisms and orientations, with several non-double couple solutions, an additional indication of fault zone complexity at depth. We further present new drone- and field-based observations of intense surface fracturing in the western rupture zone, north of the main fault plane as modeled with InSAR and GNSS data. Surface fractures exhibit "pebble-clearing" patterns mainly on the southeast side of each crack and show down-to-the-northwest vertical sense of motion; this represents a secondary fault that is below the InSAR-GNSS model spatial resolution. The obliquely-crossing fault geometry, pronounced shallow slip deficit, the distributed fractures, off-fault aftershocks and their various focal mechanisms, and the limited expression of long-term tectono-geomorphic features suggest that the MCRE ruptured along a structurally complex and immature fault system. This may reflect that the Mina deflection faults, which are thought to rotate clockwise about vertical axes, are continuously diverted away from being favorable to slip, preventing the emergence of a single through-going fault that could attain structural maturity.

RELOCATING THE UTAH MAGNA AFTERSHOCK SEQUENCE USING NonLinLoc, SOURCE-SPECIFIC STATION TERMS, AND WAVEFORM SIMILARITY

Daniel Wells, University of Utah, u0770911@utah.edu, danedwells@gmail.com
Anthony Lomax, Alomax Scientific, anthony@alomax.net
Benjamin Baker, University of Utah, ben.baker@utah.edu
Kristine Pankow, University of Utah Seismograph Stations, kris.pankow@utah.edu

ABSTRACT

On March 18, 2020, a magnitude 5.7 earthquake hit the Salt Lake Valley. This mainshock triggered a series of approximately 2600 aftershocks over the ensuing months, a small but significant number of which were felt by the local population. Using a dense geophone deployment and machine learning, an additional several thousand events were detected and located. Currently, both the mainshock and the majority of the aftershocks are suspected to have occurred on or near a deeper portion of the Wasatch fault. However, a small subset of aftershocks may have occurred on a portion of the more steeply dipping and poorly understood West Valley fault zone system, which is likely subsidiary to the Wasatch fault. Unfortunately, the catalog locations and limited number of resulting focal mechanisms for this subset of aftershocks provides only a crude constraint on the true fault structure. We attempt to relocate the University of Utah Seismograph Stations (UUSS) catalog and the machine learning catalog to better constrain the true fault structure. Preliminary relocations of the UUSS catalog using the NonLinLoc software and source specific station terms, for both 1D and 3D velocity models, suggests that the events located near the West Valley fault zone system actually occurred on the Wasatch fault. These results suggest that the Wasatch fault is minimally listric in contrast to what has been previously proposed. Future relocations will include waveform similarity to further refine absolute locations.

THE IMPLICATIONS OF A LISTRIC WASATCH FAULT FOR SESIMIC HAZARD ALONG UTAH'S WASATCH FRONT

Ivan G. Wong, Lettis Consultants International, wong@lettisci.com

Patricia A. Thomas, Lettis Consultants International, thomas@lettisci.com

James C. Pechmann, University of Utah, james.pechmann@utah.edu

ABSTRACT

Observations of the 2020 moment magnitude **(M)** 5.7 Magna earthquake suggest that the event occurred on the Warm Springs section of the Salt Lake City segment of the Wasatch fault (Figure 1). This interpretation is still uncertain, but if correct it requires a listric geometry for this section of the fault. Whether a listric Warm Springs section is representative of the whole Salt Lake City segment, and possibly more of the Wasatch fault, has significant implications for hazard and risk along the Wasatch Front. The Wasatch fault has traditionally been modeled in seismic hazard analyses as a moderately dipping (50° ± 15°) planar normal fault. This assumed fault geometry is embedded in both site-specific and regional seismic hazard analyses, including the U.S. Geological Survey National Seismic Hazard Maps, and hence the International Building Codes adopted in Utah.

To illustrate the impact of fault geometry on seismic hazard estimates in the Salt Lake Valley, we performed a probabilistic seismic hazard analysis (PSHA) for three representative sites (Figure 1) using both listric and planar Wasatch fault models. The models are from a logic tree developed during discussions with the Working Group on Utah Earthquake Probabilities (WGUEP) to address the epistemic uncertainties in the geometry of the Wasatch fault. This logic tree has four possible models for the Salt Lake City segment that are consistent with the available observations of the 2020 Magna earthquake and their uncertainties. The other inputs into the PSHA include a partially time-dependent Wasatch Front seismic source model based on the WGUEP model and the NGA-West2 ground motion models. We use an average site condition typical of the Quaternary sediments in Salt Lake Valley with a V_s30 of 300 m/sec.

The PSHA results indicate that the seismic hazard for a listric Wasatch fault relative to that of a moderately dipping planar fault increases with increasing distance from the surface trace of the Wasatch fault. On the west side of the Salt Lake Valley, the increases in probabilistic ground motions for listric models compared to planar models with 50° ± 15° dips range up to 24% for peak horizontal ground acceleration and 40% for horizontal 1.0 sec spectral acceleration. The listric models result in higher hazard in this area because of the generally shorter distances from the fault to the ground surface, combined with enhanced hanging-wall effects. Hence, if the Warm Springs section of the Salt Lake City segment is listric, the National Seismic Hazard Maps underestimate the hazard in western and central parts of the Salt Lake Valley. If other sections of the Wasatch fault are listric, the hazard has also been underestimated along parts of the adjacent Wasatch Front. This potentially increased seismic hazard has implications for seismic design and risk.

A PDF of this poster is available at the following link:

https://ugspub.nr.utah.gov/publications/misc_pubs/mp-177/mp-177-p14.pdf

Figure 1. *Sections of the west-dipping Salt Lake City segment of the Wasatch fault zone (Warm Springs, East Bench, and Cottonwood) and the east-dipping West Valley fault zone. The red lines show the surface traces of these active faults. Bold red arrows mark the Salt Lake City segment boundaries. The yellow squares mark our study sites at Temple Square, the Salt Lake City International Airport, and the town of Magna. (Figure modified from the Utah Geological Survey).*

INTERSEISMIC STRAIN ACCUMULATION ACROSS THE CENTRAL BASIN AND RANGE: IMPLICATIONS FOR SOUTHERN NEVADA SEISMIC HAZARD

Zachary M. Young, Nevada Geodetic Laboratory, zyoung@nevada.unr.edu
Corné Kreemer, Nevada Geodetic Laboratory, kreemer@unr.edu
William C. Hammond, Nevada Geodetic Laboratory, whammond@unr.edu
Geoffrey Blewitt, Nevada Geodetic Laboratory, gblewitt@unr.edu

ABSTRACT

Crustal deformation in the central Basin and Range between the Colorado Plateau and the Eastern California Shear Zone is active but slow, making it a challenge to assess how strain is distributed and crustal motion transferred. However, knowledge of strain rates is very important, particularly for addressing the seismic hazard for both the Las Vegas urban area and the site of the proposed Yucca Mountain nuclear waste repository, in southern Nevada. Global Positioning System (GPS) data provide important constraints, particularly now that the GPS network in the area has substantially expanded in recent years. However, because deformation is slow, it is important to mitigate any transient tectonic and non-tectonic signals to obtain the most accurate long-term interseismic motion and use robust estimation of strain rates. We use data from all GPS stations in the region, including both long-running continuous and semi-continuous stations. Postseismic displacements at these stations are modeled and removed using source parameters for 41 events, dating back to the 1700 Cascadia megathrust earthquake, and are found to contribute significantly to the deformation field within the central Basin and Range. While the postseismic field is dominated by a few large events, we find the cumulative contributions from events which are individually insignificant are large enough to alter the velocity gradients of the region. We also remove regionally correlated noise from the time series with the Common Mode Component Imaging technique. The removal of both the postseismic transients and common-mode noise substantially reduces the velocity uncertainties, by 62.1% in the east component and 53.8% in the north and improves the spatial coherency of the velocity field. We find deformation is active within the Las Vegas Valley with east–west extension 0.5–0.6 mm/yr. Furthermore, the interseismic strain rate field, calculated with the final velocities, reveals higher strain rates through southern Nevada than in previous studies, with rates within the Las Vegas Valley of 8.5 ± 2.4 x10^{-9} yr^{-1}. Our results confirm shear along the Pahranagat Shear Zone but the estimated amplitude is strongly affected by postseismic relaxation.

A PDF of this poster is available at the following link:

https://ugspub.nr.utah.gov/publications/misc_pubs/mp-177/mp-177-p15.pdf

3D SHEAR WAVE VELOCITY MODEL OF SALT LAKE VALLEY VIA SURFACE WAVES RECORDED BY THE MAGNA AFTERSHOCK NODAL ARRAY

Qicheng Zeng, University of Utah, Qicheng.Zeng@utah.edu
Fan-Chi Lin, University of Utah, FanChi.Lin@utah.edu
Amir A. Allam, University of Utah, amir.allam@utah.edu

ABSTRACT

We deployed 168 three-component nodal geophones across Salt Lake Valley between March 18 and April 30 in 2020, in response to the M 5.7 Magna earthquake. On March 31, 2020, a M6.5 earthquake struck central Idaho. In this study, we aim to construct a 3D shear velocity model of Salt Lake Valley using Rayleigh waves excited by the Idaho earthquake and observed across the temporary nodal array as well as 49 stations of the regional network. We show that Rayleigh wave ellipticity or horizontal to vertical (H/V) ratios between 10 and 20 sec period can be measured using the direct Rayleigh wave. Moreover, we show that additional H/V ratios can be measured down to a 5 sec period using the multi-component earthquake coda cross-correlations. Clear correlations are observed between the measured H/V ratios and known basin structure, where high H/V ratios are observed in areas associated with thick unconsolidated sediments. Taking advantage of the outstanding shallow sensitivity of the H/V ratios, we invert for a 3D Vs model of the Salt Lake Valley with homogeneous Rayleigh wave phase velocities between 5 and 20 sec period as additional constraints for deeper structure. Our model complements the current Community Velocity Model (CVM), which is mostly constrained by borehole and gravity measurements, and opens up future opportunities to update the CVM that is critical for regional seismic assessment.

A PDF of this poster is available at the following link:

https://ugspub.nr.utah.gov/publications/misc_pubs/mp-177/mp-177-p16.pdf

EARTHQUAKE EARLY WARNING – DAY 3

Poster Session - Abstracts

NOTA Realtime GNSS data for Earthquake Response in the Basin and Range; *Sarah Doelger, UNAVCO, Inc.*

NOTA REALTIME GNSS DATA FOR EARTHQUAKE RESPONSE IN THE BASIN AND RANGE

Brendan Hodge, UNAVCO Inc., hodge@unavco.org
Sarah Doelger, UNAVCO Inc., doelger@unavco.org
Tim Dittmann, UNAVCO Inc., dittmann@unavco.org

ABSTRACT

Geodetic study of the Basin and Range has been supported by UNAVCO for over three decades. One of the first regional GPS networks to continuously measure extension rates of the Basin and Range was the BARGN (Basin and Range Geodetic Network) installed by UNAVCO in the late 1990s that later became part of a nucleus network for the Plate Boundary Observatory (PBO). Currently UNAVCO operates many of the original BARGN and PBO stations as part of the Network of the Americas (NOTA). NOTA is a core component of the NSF Geodetic Facility for the Advancement of Geoscience (GAGE), operated by UNAVCO. In recent years, UNAVCO has been upgrading the NOTA network in order to provide full GNSS (Global Navigation Satellite Systems) data availability and real-time 1 Hz GNSS data products. Realtime stations in NOTA typically have data latency less than 1 second arriving at the data processing center. The extent of NOTA includes densely populated areas around Salt Lake City, Utah, and Reno, Nevada. The NOTA station density in these populated areas provides geodetic data for future earthquake early warning efforts. In the event of a medium-large earthquake (~>M6.0), real-time position displacement data is utilized for rapid event magnitude estimation and measurement of coseismic displacement. UNAVCO also downloads high-rate 5-sps (5 Hz) data from all available NOTA GPS/GNSS stations within the area of anticipated coseismic surface displacement for post-processing. The use of real-time GNSS data allows for a geodetic-derived earthquake magnitude estimate within tens of seconds of the event. A case study from the M6.5 Monte Cristo Range earthquake on May 15, 2020, highlights the utility of real-time high-rate data for quickly derived earthquake magnitude even in areas of relatively low station density.

A PDF of this poster is available at the following link:

https://ugspub.nr.utah.gov/publications/misc_pubs/mp-177/mp-177-p17.pdf

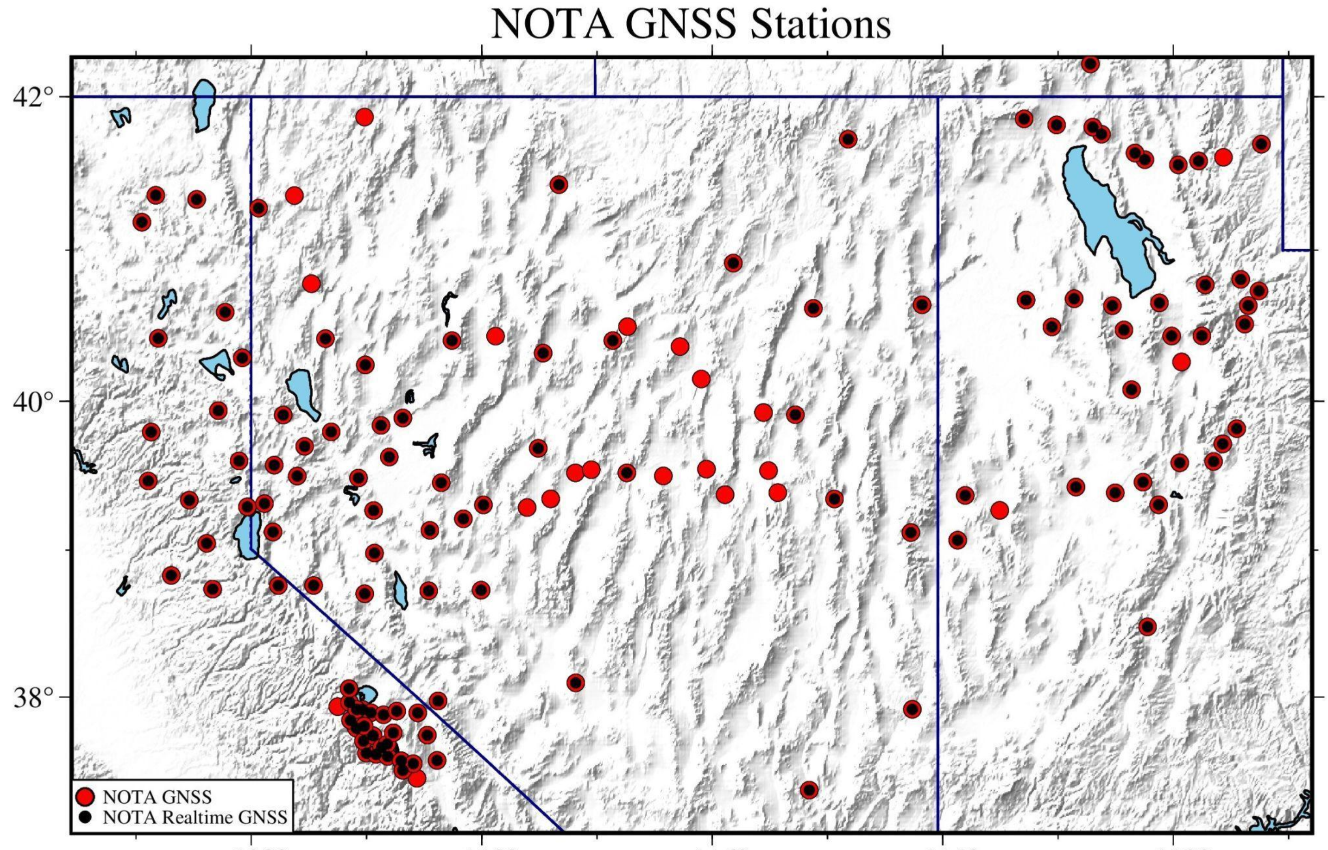

Figure 1. *NOTA GNSS stations located within the Basin and Range and vicinity.*